Nat. Hazards Earth Syst. Sci. Discuss., 3, 4159–4187, 2015
www.nat-hazards-earth-syst-sci-discuss.net/3/4159/2015/
doi:10.5194/nhessd-3-4159-2015
© Author(s) 2015. CC Attribution 3.0 License.

Natural Hazards and Earth System Sciences
Open Access
Discussions

This discussion paper is/has been under review for the journal Natural Hazards and Earth System Sciences (NHESS). Please refer to the corresponding final paper in NHESS if available.

Behavior analysis by model slope experiment of artificial rainfall

M. C. Park

Kumoh National Institute of Technology, Gumi-si, Republic of Korea

Received: 14 April 2015 – Accepted: 14 May 2015 – Published: 22 June 2015

Correspondence to: M. C. Park (xlage0@naver.com)

Published by Copernicus Publications on behalf of the European Geosciences Union.

Abstract

In this study, we performed a model slope experiment with rainfall seepage, and the results were compared and verified with the unsaturated slope stability analysis method. In the model slope experiment, we measured the changes in water content and matric suction due to rainfall seepage, and determined the time at which the slope failure occurred and the shape of the failure. In addition, we compared and verified the changes in the factor of safety and the shape of the failure surface, which was calculated from the unsaturated slope stability analysis with the model experiment. From the results of experiment and analysis, it is concluded that the unsaturated slope stability analysis can be used to accurately analyze and predict rainfall-induced slope failure. It is also concluded that in seepage analysis, setting the initial conditions and boundary conditions is very important. If engineers will use the measured pore water pressure or matric suction, the accuracy of analysis can be enhanced. The real-time monitoring system of pore water pressure or matric suction can be used as a warning of rainfall-induced slope failure.

1 Introduction

Recently, there have been many natural disasters due to climate changes. Especially, slope failure in downtown areas has caused loss of lives and of property. The causes of slope failures around the world are: intense rainfall, rapid snow melt, water level changes in rivers or lakes at the foot of slopes, volcanic eruptions, and earthquakes (Wieczorek, 1996). Among these, slope failure resulting from rainfall is the most frequent one in the case of Korea, where there are four seasons each year, and which is located within a mid-latitude region not prone to earthquakes. Slope failure is frequently due to antecedent rainfall, a rainy spell effect in summer, and freezing and thawing in the spring (Oh and Lu, 2015).

NHESSD

3, 4159–4187, 2015

CC BY

When evaluating slope stability, geology, hydraulics, hydrology and soil mechanics are all taken into account. Geologically, the cause of slope failure takes into account the orientation of the joint plane, which is weak ground and is especially important in the rock slope. As regards hydraulics and hydrology, the external forces that influence slope stability include the groundwater table and rainfall. In a slope stability analysis, the following are used: either (1) the method for determining and analyzing the groundwater table, or (2) the method for considering the seepage of rainfall.

When considering a groundwater table, we assume that it is located on the inclined plane of a slope, leading to a design that is very conservative and excessive. When considering the effects of rainfall, we take into account the geographical conditions, drainage conditions, and the regional rainfall intensity and duration determined by the design frequency, while performing seepage and slope stability analysis. The unsaturated slope design method can be analyzed more accurately or less conservatively than the traditional method (Oh and Lu, 2015).

In soil mechanics, the causes of a slope failure are pore water pressure and water content, which reduce the shear strength of a slope or increase the shear stress (Brand, 1981; Brenner et al., 1985). In a traditional slope stability analysis, cohesion and internal friction angle under saturation are applied to calculate the shear strength, and the strength parameters under unsaturation are applied when considering the rainfall seepage. However, there are the limitations of restricted geotechnical survey, inhomogeneity and anisotropy of the soil slope (Oh and Lu, 2015). Also, an intense rainfall differs from the conditions included in the design, and can occur due to an abnormal climate change. Because of these limitations, slope failure can occur (Tohari et al., 2007).

In general, rainfall-induced slope failures are caused by increased pore pressure and seepage force during periods of intense rainfall (Anderson and Sitar, 1995; Sidle and Swanston, 1982; Wang and Sassa, 2003; Sitar et al., 1993). Previous studies have been conducted to understand the failure mechanism of a slope, and to determine the point of initiation of failure. Until now, the process of slope failure is not clear (Regmi et al., 2014; Tohari et al., 2007).

NHESSD
3, 4159–4187, 2015

CC BY

Recently, field measurements and laboratory experiments on model slopes have been conducted in order to understand the process of slope failure and seepage under rainfall. The studies of field measurements used pore water pressure because it is easy to measure and it is the most important factor in the process of the slope failure (Johnson and Sitar, 1990; Rahardjo, 2005). However, it is difficult to generalize about the process of rainfall-induced slope failure because the mechanism and behavior of pore water pressure depends in each case on the hydrology, topography and soil properties of the slope (Sitar et al., 1993).

Laboratory experiments were conducted in order to understand the process of slope failure, to monitor pore water pressure, soil suction, groundwater depth and slope deformation, and the failure surface within a slope (Fukuzono, 1987; Regmi et al., 2014; Yagi and Yatabe, 1987; Kitamura, 1999; Yokota et al., 2000; Sasahara, 2001; Tohari et al., 2007).

Slope stability is calculated by using the ratio of shear strength and shear stress that occurs along the failure surface. In traditional slope stability analysis, the saturated strength parameters are applied by assuming the worst case, and the groundwater table is located on the inclined plane of a slope during the wet season. However, when rainfall seepage is considered, then since the weight of the soil increases due to the seepage of water, the shear stress is increased and the matric suction is decreased, which leads to a decrease in shear strength. As a result, the factor of safety dramatically decreases. Especially when it happens around the failure surface, the soil around the failure surface loses its shear strength, leading to a collapse.

In this study, we performed a model slope experiment to understand the process of water seepage and slope failure caused by rainfall; and we compared and verified the results with unsaturated slope stability analysis. In the model slope experiment, we created artificial rainfall on a slope and measured the changes in water content, which acts as a load factor during seepage, and the change of matric suction, which acts as a resistance factor. Also, we identified the time and the shape of slope failure after the rainfall seepage.

NHESSD
3, 4159–4187, 2015

CC BY

Unsaturated slope stability analysis was used to calculate the change in the factor of safety due to rainfall seepage, by performing seepage analysis and the limit equilibrium method. Seepage analysis was performed under an unsteady state due to rainfall, and the factor of safety was calculated from the calculated head value. We compared and verified the changes in the factor of safety, as well as the time and shape of the slope failure resulting from the rainfall, with the results from the model experiment.

2 Material and methods

The experiment devices consisted of a soil container (2.0 m × 1.0 m × 0.6 m), an artificial rainfall simulator, and a measuring device. A 5 cm drainage layer was formed with crushed stones in the bottom layer of a slope. This was done in order to ensure that slope failure occurred only when there was a change in the shear strength of the slope due to rainfall seepage.

In the slope model experiment by Tami et al. (2004), seepage flow changed due to the soil layer with a relatively small of permeability, located at the bottom of a slope. In the experiments of Tohari et al. (2007) and Regmi et al. (2014), the elevated groundwater table caused the failure surface to form at the toe of a slope. In this study, we eliminated these influences and considered only a slope failure occurring due to rainfall seepage.

In the soil container, a finite slope with a height of 60 cm and inclination of 70° was formed. The slope was constructed uniformly, using plywood and tamper, with the degree of compaction being 85 % and the height 20 cm. It was formed in three layers.

We used weathered granite soil, which is the soil most prevalent in the mountainous terrains of Korea. According to the unified soil classification system, it was designated as SW, with a specific gravity of 2.53, effective grain size of 7.57 mm, and coefficient of uniformity of 0.25 mm. In the compaction test, the maximum dry unit weight and the optimal water content were calculated to be 18.95 kN m^{-3} and 11.50 %, respectively. In the direct shear test carried out under the same conditions as for the model slope,

CC BY

cohesion was 0 kPa and the internal friction angle was 36.9°. The saturated coefficient of permeability of the constant-head method was calculated to be 0.013 $cm\,s^{-1}$.

To determine the creation process of a rainfall-induced slope failure, we measured the water content, which acts as a load factor during seepage, and the matric suction, which acts as a resistance factor.

Water content was measured using a TDR (Time Domain Reflectometer) sensor. The TDR sensor uses the association between the dielectric constant and water content (Topp et al., 1980). Electrical pulses from the TDR measuring device go through a probe and are then changed by water content. After a simple correction process, we found the value for the water content. The probe for the TDR sensor was the EC-5 from Decagon Devices Inc., and its dimensions are 8.9 cm × 1.8 cm × 1.7 cm (Devices, 2006; Bogena et al., 2007). We performed the correction process with weathered granite soil, with the degree of accuracy being ±3 % and the resolution 0.1 %. The data logger used was an Em50 from Decagon Devices, measuring every five minutes.

We measured matric suction using a tensiometer, which consists of a porous ceramic pipe and a transducer. The porous ceramic pipe was a Jet Fill Tensiometer from Soilmoisture, and the pressure sensor was a Tensiometer Transducer from ICT International Pty Ltd. (Indrawan et al., 2012). In the Jet Fill Tensiometer, pore water pressure is created from the surface tension of water at the contact point between a porous ceramic cup and the soil, and it is measured by the pressure sensor. The measuring range of the pressure sensor is $0 \sim -100$ kPa, with a resolution of 0.1 kPa and a degree of accuracy of ±1.0°. The data logger used was LogoSens from OTT Hydrometric, and the measurements were taken every five minutes.

The water content and matric suction sensors were installed in four locations. Sensor A was placed 10 cm above the slope toe and 50 cm from the top of the slope, where the rainfall seepage occurs. Sensor B was placed 35 cm from the top of the slope, and sensors C and D were placed 20 cm from the top of the slope.

A rainfall simulator was set approximately 50 cm above the surface of the model slope. The rainfall simulator was controlled to provide artificial rainfall with an intensity

NHESSD
3, 4159–4187, 2015

CC BY

of 30 mm h^{-1} on the upper surface (1.0 m × 1.0 m) of the model slope. The artificial rainfall would introduce surface erosion and the formation of gullies. The amount of water flowing into the sprayer arms was carefully controlled, and monitored through a flow meter.

Unsaturated slope stability analysis was carried out with seepage analysis and slope stability analysis. Seepage analysis under the unsteady conditions was performed first, and the factor of safety was calculated with the limit equilibrium method, by applying the water head value inside the slope to the slope stability analysis.

For slope stability analysis under transient unsaturated seepage conditions using the hydromechanical framework, only three additional parameters are needed. These are the residual water content θ_r, the air entry pressure u_b, and the pore size distribution parameter n. The SWRCs were obtained from the pressure plate tests and fit to the van Genuchten model using the RETC code (Van Genuchten, 1980). Direct shear tests were conducted under saturated conditions in order to obtain shear strength parameters for the soil. As shown in Fig. 3a and Table 2, the air entry pressures u_b are 0.452 kPa, the pore size distribution parameter n is 1.189, the residual water content θ_r is 0, and the saturated volumetric water content θ_s is 0.38.

The hydrological behavior due to infiltration of the artificial rainfall was analyzed numerically using the SEEP/W module of Geostudio 2007 (Krahn, 2007). The geometry of the model slope for numerical analysis was as in Fig. 4. Meshing was done with the combination of quadrangles and triangles, with the element size around 3 cm, which is segmented into 942 nodes and 853 elements. In seepage analysis, setting the initial conditions and boundary conditions is very important.

To analyze the unsteady state, we input the matric suction that was measured from the experimental process using the spatial function. The boundary condition of 30 mm h^{-1} of rainfall was applied only to the top of the slope, which was the same as in the model experiment. The inclination plane of the slope was set such that the seepage water could flow out. On the left, right, and bottom sides, an impervious boundary was placed, and the face of the layer of crushed stones was also set such that the seep-

Discussion Paper | Discussion Paper | Discussion Paper | Discussion Paper |

NHESSD

3, 4159–4187, 2015

Behavior analysis by model slope experiment of artificial rainfall

M. C. Park

age water could flow out. The results of the seepage analysis is of unsteady states, so they are shown as the total stress, pore water pressure, and the water content with the changes in time; and they were applied to the slope stability analysis.

In the slope stability analysis, the limit equilibrium method was used, which the design standards have presented. It was determined by the ratio of shear stress and shear strength along the failure surface. The factor of safety was calculated with Eq. (1).

$$\mathrm{FOS} = \frac{\sum_i (\tau_f l_{\mathrm{base}})_i}{\sum_i (\tau l_{\mathrm{base}})_i} = \frac{\sum_i \left[(c' + \sigma' \tan \varnothing') l_{\mathrm{base}}\right]_i}{\sum_i (\tau l_{\mathrm{base}})_i} \tag{1}$$

where i is the slice index and l_{base} is the base length of each slice, τ_f and τ are respectively the shear strength and shear stress, c' is the drained cohesion and $\varnothing'$ is the drained friction angle.

The factor of safety was calculated numerically using the SLOPE/W module of Geostudio 2007 (Geo-slope, 2007). The suction stress and the effective stress are incorporated into the shear strength in the SLOPE/W module as follows:

$$\tau_f = c' + \sigma' \tan \varphi' = c' + \left\{ (\sigma - u_a) + \frac{\theta - \theta_\mathrm{r}}{\theta_\mathrm{s} - \theta_\mathrm{r}} (u_a - u_w) \right\} \tan \varphi'. \tag{2}$$

3 Results and discussion

Figure 5 and Table 3 show the measured water content due to artificial rainfall seepage. Simulated artificial rainfall of 30 mm h^{-1} began 180 min after the water content was measured. After 320 min, model slope failure occurred. Depending on the depth of TDR sensor installation, there were differences in the time that the movement started.

For sensor A, which was installed 50 cm from the top of the slope (10 cm above the slope toe), volumetric water content rapidly increased 120 min after the rainfall simulation began. Slope failure occurred 20 min after the volumetric water content increased

CC BY

in sensor A. For sensors B through D, which were placed 20 to 35 cm from the top, volumetric water content increased almost vertically 50 to 80 min after the rainfall simulation began, and the increase slowed down 20 to 30 min after that. At the slope failure, sensors C and D, which were placed 20 cm from the top, were close to the saturated water content of 38 %. The other sensors showed unsaturated water content. Therefore, we know that the slope failure happened before the area around the failure surface was completely saturated.

According to the experimental cases of Regmi et al. (2014) and Tohari et al. (2007), when the groundwater table existed on the toe of the slope, slope failure occurred at the saturation; but when the groundwater table did not have an effect, slope failure occurred around the toe area of the slope before saturation.

Figure 6 and Table 4 show the measured matric suction according to rainfall seepage. The simulated rainfall of 30 mm h^{-1} began 180 min after measuring the model slope, and the slope failure occurred after 320 min. For sensor A, which was installed 50 cm from the top of the slope (10 cm above the slope toe), matric suction decreased 100 min after the rainfall simulation began. Slope failure occurred 40 min after the decrease in matric suction. As shown in Fig. 6, water content increased dramatically, but the matric suction decreased slowly compared to the increase in water content. Matric suction decreased continuously until the slope failure occurred at about 5 kPa.

As seen with the water content measurement results, the failure of model slope happened when the area around the failure surface was unsaturated. In sensors B and F, which were placed at the center of the slope, rainfall seeped through the Tensiometer cable, leading to noise appearing between 180 and 260 min of measurement (Fig. 4b and f).

Figure 7 compares the changes in the water contents of the model slope experiment and the numerical analysis.

For sensor A, which was placed 50 cm from the top, the water content increased at the same time, but there was a difference in the amount of the increase (Fig. 7a). For the model slope experiment, slope failure occurred about 30 min after the water content increased at sensor A.

For sensor B, which was placed 35 cm from the top, water content increased 50 min later in the numerical analysis than in the model experiment. The amount of increase also appeared to be different (Fig. 7b).

For sensor C, which was placed 20 cm from the top, the amount of increase in water content and the time at the start of the increase were about the same (Fig. 7c). In the numerical analysis, the seepage behaviors were the same for sensors C and D, which were placed at the same depth. However, in the model slope experiment, slope failure occurred later in sensor D (Fig. 7d). In the numerical analysis, water content was increased relatively gently compared to the model experiment.

For all of the sensors, the amount of increase in the water content was about the same. The early measurement of water content was 17 %. It increased to about 35 %, due to rainfall seepage, and stayed about constant until the slope failure.

Figure 8 compares the changes in matric suction in the model slope experiment and the numerical analysis.

For sensor A, which was placed 50 cm from the top, the amount of decrease and the time at the start of the decrease were about the same, which was similar to the changes in water content (Fig. 8a).

For sensor B, which was placed 35 cm from the top, matric suction started decreasing 75 min later in the numerical analysis than in the model experiment (Fig. 8b). In the numerical analysis, matric suction continuously decreased, due to rainfall seepage, until converging to 0 kPa at 165 min. Slope failure occurred 210 min after the rainfall simulation began. When matric suctions at the time of slope failure are compared, matric suction in the model slope experiment was measured to be about 5 kPa, and about 0.2 kPa in the numerical analysis, which shows that slope failure happened at a higher matric suction in the model slope experiment.

Figure 9 shows changes in the factor of safety in the unsaturated slope stability analysis. Forty minutes after the rainfall simulation began, the factor of safety started

NHESSD
3, 4159–4187, 2015

decreasing dramatically, dropping to below one (slope failure) after about 130 min. In the model slope experiment, slope failure happened 140 min after the rainfall simulation began. Slope failure occurred 10 min earlier in the unsaturated slope stability analysis.

Figure 10 compares the failure shape in the model slope experiment and in the unsaturated slope stability analysis.

In the unsaturated slope stability analysis, the simulated failure surface showed a toe failure shape. In the model experiment, the slope failure showed an arc formation with multiple tensile cracks, which measured 16 cm parallel along the slope crown and 45 cm down from the crown. When the actual failure surface and the simulated failure surface were compared, both showed an arc form of failure, while the actual failure surface appeared as a smaller shape inside the slope, compared to the simulated failure surface with a toe failure shape. If the failure mass of the slope is retained by a fixed support at its toe, there may be some displacement with very slow movement in the head reach of the failure mass (Regmi et al., 2014).

The results demonstrated that the water content increased drastically due to rainfall seepage, and matric suction decreased at a slower pace than the water content. In the numerical analysis, the seepage behavior of matric suction was almost the same as in the experiment, but the amount and the rate of increase in water content due to rainfall seepage were lower than in the experiment. In the end, this acted as a factor determining the shape of failure and the differences in slope failure time. The factor of safety in an unsaturated slope is shown as a ratio of load factor and shear resistance factor, inputting the distribution of total head calculated from seepage analysis.

When the model experiment and the numerical analysis are compared, the behavior of matric suction, which acts as a shear resistance factor, appeared to be almost the same at points A and B; but at points C and D it showed a faster behavior in numerical analysis. As a consequence, slope failure occurred more quickly in the numerical analysis than in the model experiment.

NHESSD
3, 4159–4187, 2015

cc BY

4 Summary and conclusions

In this study, we performed a model slope experiment with rainfall seepage, and the results were compared and verified with the unsaturated slope stability analysis method. In the model slope experiment, we measured the changes in water content and matric suction due to rainfall seepage, and determined the time at which the slope failure occurred and the shape of the failure. In addition, we compared and verified the changes in the factor of safety and the shape of the failure surface, which was calculated from the unsaturated slope stability analysis with the model experiment.

The conclusions from this study are as follows.

1. In the model slope experiment, rainfall seepage caused the water content to increase dramatically and matric suction to decrease more gradually than water content, leading to the area around the failure surface collapsing at around 5 kPa. Model slope failure occurred when the bottom of the failure surface was unsaturated.

2. In seepage analysis, compared to the model experiment, water content increased relatively gradually, and seepage behaviors were about the same across all the sensors. Early water content was analyzed to be 17 %, which is higher than the results from the experiment. It increased due to rainfall seepage until it reached 35 % and remained constant until slope failure. For matric suction, seepage behaviors were about the same as the experimental results, in terms of the time of matric suction decrease and the amount of the decrease.

3. Slope failure began 140 and 130 min after rainfall simulation began in the model slope experiment and the unsaturated slope stability analysis, respectively. In the numerical analysis, the failure started 10 min earlier. To describe the shape of failure: in the model experiment, the slope failure showed an arc formation with multiple tensile cracks, which measured 16 cm parallel along the slope crown and 45 cm down from the crown. In the unsaturated slope stability analysis, the simu-

Discussion Paper | Discussion Paper | Discussion Paper | Discussion Paper |

NHESSD

3, 4159–4187, 2015

Behavior analysis by model slope experiment of artificial rainfall

M. C. Park

cc BY

lated failure surface showed a toe failure shape. When the actual failure surface and the simulated failure surface are compared, both showed an arc form of failure, while the actual failure surface appeared as a smaller shape inside the slope, compared to the simulated failure surface with a toe failure shape.

4. The results of the experiment showed that water content increased dramatically due to rainfall seepage, and matric suction decreased more gradually than the water content. In the numerical analysis, the seepage behavior of matric suction was almost the same as in the experiment; but the amount and the rate of increase in water content due to rainfall seepage were lower than in the experiment. In the end, this acted as a factor determining the shape of failure and the differences in slope failure time.

From the results of the experiment and the analysis, it is concluded that the unsaturated slope stability analysis can be used to accurately analyze and predict rainfall-induced slope failure. In seepage analysis, setting the initial conditions and boundary conditions is very important. If engineers will use the measured pore water pressure or matric suction, the accuracy of analysis can be enhanced. The real-time monitoring system of pore water pressure or matric suction can be used as a warning of rainfall-induced slope failure.

Acknowledgements. This research was supported by a grant (15SCIP-B065985-03) from the Smart Civil Infrastructure Research Program funded by the Ministry of Land, Infrastructure and Transport (MOLIT) of the Korean government, and Korea Agency for Infrastructure Technology Advancement (KAIA).

References

Anderson, S. A. and Sitar, N.: Analysis of rainfall-induced debris flows, J. Geotech. Eng.-ASCE, 121, 544–552, 1995.

Bogena, H., Huisman, J., Oberdörster, C., and Vereecken, H.: Evaluation of a low-cost soil water content sensor for wireless network applications, J. Hydrol., 344, 32–42, 2007.

Brand, E.: Some thoughts on rain-induced slope failures, in: Proceedings of the 10th International Conference on Soil Mechanics and Foundation Engineering, Stockholm, 1981.
Brenner, R., Tam, H., and Brand, E.: Field stress path simulation of rain-induced slope failure, in: Proceedings of 11th International Conference on Soil Mechanics and Foundation Engineering, San Francisco, 1985.
Decagon Devices: ECH2O Soil Moisture Sensor: Operators Manual for Models EC-20, EC-10 and EC-5 (Version 5), Decagon Devices Inc., Pullman, Wash., 2006.
Fukuzono, T.: Experimental study of slope failure caused by heavy rainfall, erosion and sedimentation in the Pacific Rim, in: Proceedings of the Corvallis Symposium, August 1987, Corvallis, 1987.
Indrawan, I. G. B., Rahardjo, H., Leong, E. C., Tan, P. Y., Fong, Y. K., and Sim, E. K.: Field instrumentation for monitoring of water, heat, and gas transfers through unsaturated soils, Eng. Geol., 151, 24–36, 2012.
Johnson, K. and Sitar, N.: Hydrologic conditions leading to debris-flow initiation, Can. Geotech. J., 27, 789–801, 1990.
Kitamura, R., Jomoto, K., Yamamoto, K., Terachi, T., Abe, H., and Iryo, T.: Field measurement of suction in soil and rainfall in Kagoshima Prefecture, in: Proceedings, 1st International Symposium on Slope Stability Engineering, Shikoku, 1999.
Krahn, J.: Seepage Modeling with SEEP/W 2007: an Engineering Methodology, Geo-slope International Ltd Printed, Alberta, 2007.
Oh, S. and Lu, N.: Slope stability analysis under unsaturated conditions: case studies of rainfall-induced failure of cut slopes, Eng. Geol., 184, 96–103, 2015.
Rahardjo, H., Lee, T. T., Leong, E. C., and Rezaur, R. B.: Response of a residual soil slope to rainfall, Can. Geotech. J., 42, 340–351, 2005.
Regmi, R. K., Jung, K., Nakagawa, H., and Kang, J.: Study on mechanism of retrogressive slope failure using artificial rainfall, Catena, 122, 27–41, 2014.
Sasahara, K.: Mechanical model for prediction of steep sandy slope failure due to rainfall using surface displacement, Tsuchi-to-Kiso, 49, 13–15, 2001.
Sidle, R. and Swanston, D.: Analysis of a small debris slide in coastal Alaska, Can. Geotech. J., 19, 167–174, 1982.
Sitar, N., Anderson, S. A., and Johnson, K. A.: Conditions for initiation of rainfall-induced debris flows, Stability and performance of slopes and embankments II, Geotechnical Special Publication (GSP) No. 31, ASCE, 834–849, 1993.

NHESSD
3, 4159–4187, 2015

Behavior analysis by model slope experiment of artificial rainfall

M. C. Park

CC BY

Tami, D., Rahardjo, H., and Leong, E. C.: Effects of hysteresis on steady-state infiltration in unsaturated slopes, J. Geotech. Geoenviron., 130, 956–967, 2004.

Tohari, A., Nishigaki, M., and Komatsu, M.: Laboratory rainfall-induced slope failure with moisture content measurement, J. Geotech. Geoenviron., 133, 575–587, 2007.

Topp, G., Davis, J., and Annan, A. P.: Electromagnetic determination of soil water content: measurements in coaxial transmission lines, Water Resour. Res., 16, 574–582, 1980.

Van Genuchten, M. T.: A closed-form equation for predicting the hydraulic conductivity of unsaturated soils, Soil Sci. Soc. Am. J., 44, 892–898, 1980.

Wang, G. and Sassa, K.: Pore-pressure generation and movement of rainfall-induced landslides: effects of grain size and fine-particle content, Eng. Geol., 69, 109–125, 2003.

Wieczorek, G. F.: Landslide triggering mechanisms, in: Landslide: Investigarion and mitigation (Special Report), edited by: Turner, A. K. and Schuster, R. L., Special Report 247, National Research Council, Transportation and Research Board, Washington, D.C., 76–90, 1996.

Yagi, N. and Yatabe, R.: Prediction method of slope failure in sandy soil due to rainfall, in: Proceedings, 8th Asian Regional Conference on Soil Mechanics and Foundation Engineering, Kyoto, 1987.

Yokota, S., Iwamatsu, A., Imura, R., Matsuyuki, K., and Ohkawa, T.: A new warning index for debris flows based on rainfall and groundwater depth, in: Proceedings, GeoEng2000: an International Conference on Geotechnical and Geological Engineering, Melbourne, 2000.

CC BY

Table 1. Physical properties of soil.

G_s		2.53	PL (%)	–
Compaction test	$\gamma_{d,\,max}$ (kN m^{-3})	18.95	D_{10} (mm)	0.25
	OMC (%)	11.50	D_{30} (mm)	0.78
Sand replacement method	Dry unit weight γ_d (kN m^{-3})	16.05	D_{60} (mm)	1.87
	w (%)	8.42	Gravel (%)	6.05
k_s (cm s^{-1})		0.013	Coarse sand (%)	78.80
Triaxial compression test	Cohesion (kPa)	0.0	Fine sand (%)	13.20
	Internal friction (°)	36.9	Silty (%)	2.00
Uniformity coefficient C_u		7.47	USCS	SW
Coefficient of curvature C_c		1.32	–	

NHESSD
3, 4159–4187, 2015
Behavior analysis by model slope experiment of artificial rainfall
M. C. Park

CC BY

NHESSD
3, 4159–4187, 2015

Behavior analysis by model slope experiment of artificial rainfall

M. C. Park

CC BY

Table 2. Geotechnical and hydraulic properties of model slope.

Analysis parameter	Seepage Soil	Crushed stone	Slope parameter	Soil	Crushed stone
u_b (kPa)	0.452	–	γ_t (kN m^{-3})	16.05	19.00
n	1.189	–	c' (kPa)	0	0
θ_s (%)	0.38	–	$\varnothing'$ (°)	36.9	45.0
θ_r (%)	0				
k_s (m s^{-1})	1.30×10^{-4}	0.13	–	–	–

Table 3. Variation of volumetric water content.

Parameter		A	B	C	D
Initial water content (%)		4.60	3.75	6.89	5.79
Time until seepage (min)		120	80	45	65
Failure after seepage	Time (min)	20	60	95	75
	VWC_{max} (%)	27.63	28.06	36.99	34.78
	VWC_{var} (%)	23.03	24.31	30.10	28.99

NHESSD
3, 4159–4187, 2015

Behavior analysis by model slope experiment of artificial rainfall

M. C. Park

CC BY

Table 4. Variation of matrix suction.

Parameter		A	B	C	D
Initial matric suction (kPa)		30.35	36.04	31.38	30.77
Time until seepage (min)		100	–	45	45
Failure after seepage	Time (min)	40	–	95	95
	$(u_a - u_b)_{\text{min}}$ (kPa)	4.87	4.86	6.19	5.93
	$(u_a - u_b)_{\text{var}}$ (kPa)	25.48	31.18	25.19	24.84

NHESSD
3, 4159–4187, 2015

CC BY

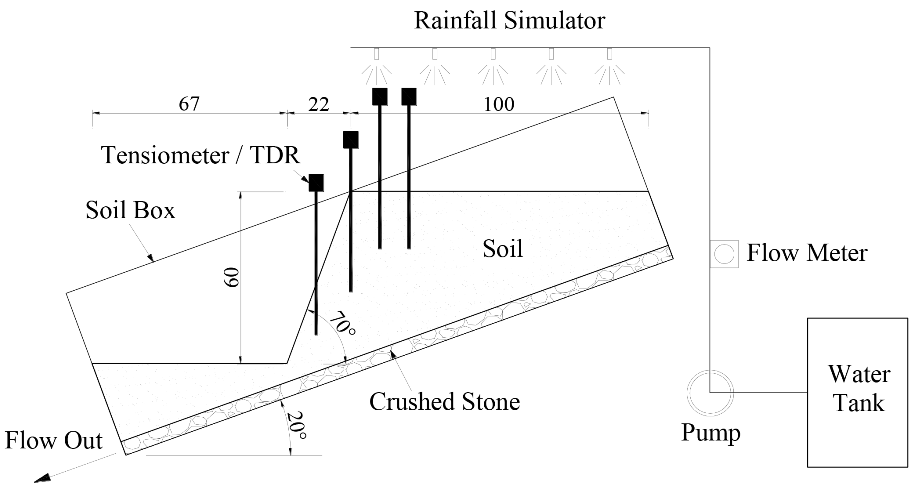

Figure 1. Experimental set up in Kumoh national institute of technology, Korea.

NHESSD
3, 4159–4187, 2015

Behavior analysis by model slope experiment of artificial rainfall

M. C. Park

Title Page
Abstract | Introduction
Conclusions | References
Tables | Figures
◀| |▶
◀ ▶
Back | Close
Full Screen / Esc
Printer-friendly Version
Interactive Discussion

CC BY

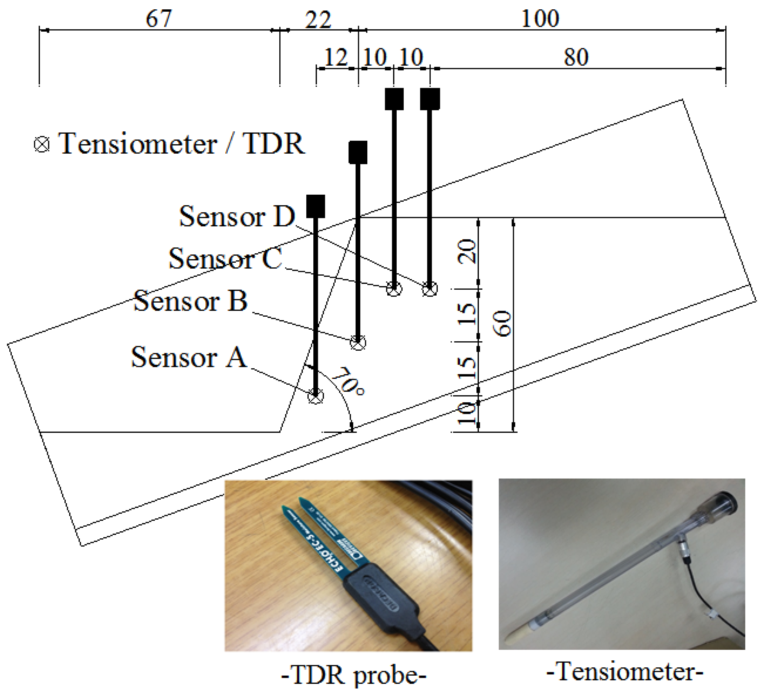

Figure 2. Model slope with arrangement of TDR and tensiometer.

NHESSD
3, 4159–4187, 2015

Title Page
Abstract | Introduction
Conclusions | References
Tables | Figures
◀I | ▶I
◀ | ▶
Back | Close
Full Screen / Esc
Printer-friendly Version
Interactive Discussion

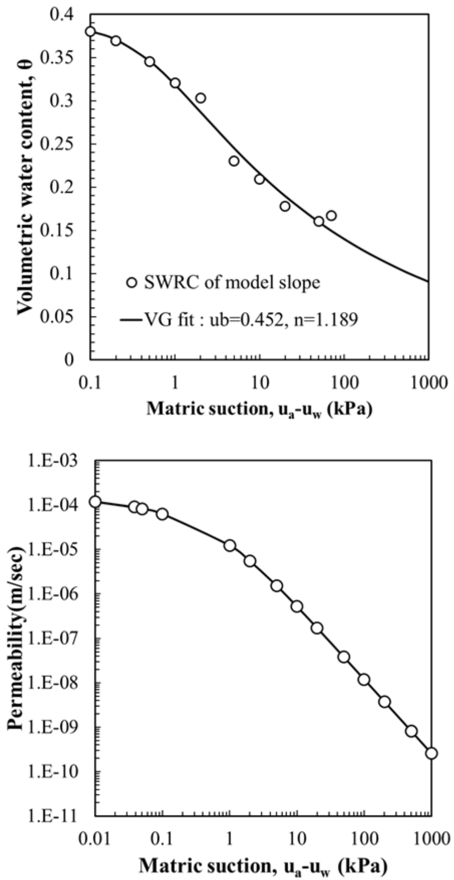

Figure 3. Hydro-mechanical properties of: **(a)** soil water retention data, **(b)** hydraulic conductivity function.

CC BY

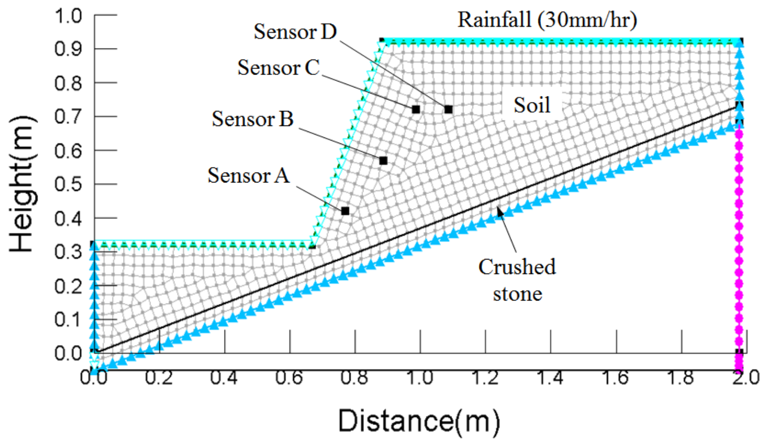

Figure 4. Geometry and boundary condition of model slope.

NHESSD

3, 4159–4187, 2015

Behavior analysis by model slope experiment of artificial rainfall

M. C. Park

CC BY

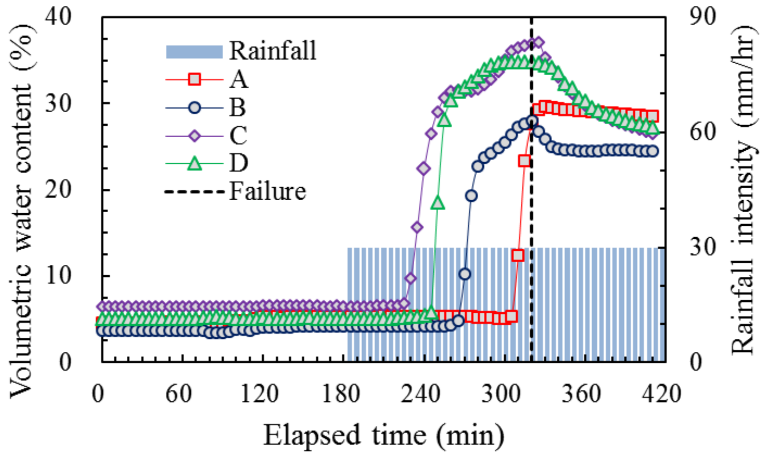

Figure 5. Variation of volumetric water content in experiment.

NHESSD
3, 4159–4187, 2015

Behavior analysis by model slope experiment of artificial rainfall

M. C. Park

Title Page
Abstract Introduction
Conclusions References
Tables Figures
Back Close
Full Screen / Esc
Printer-friendly Version
Interactive Discussion

CC BY

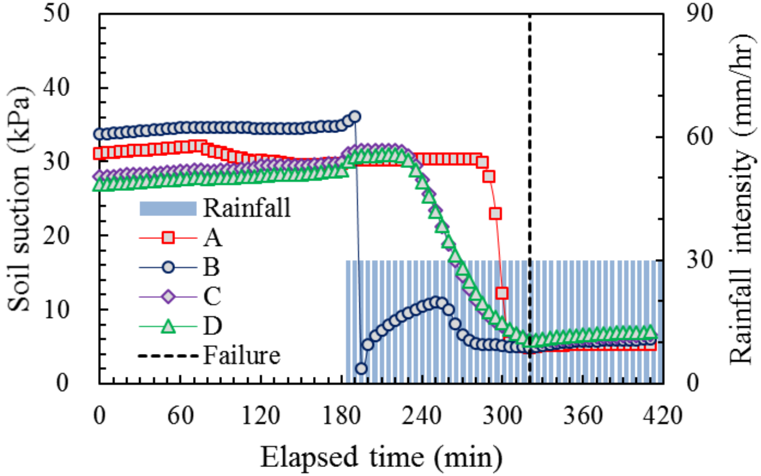

Figure 6. Variation of soil suction in experiment.

NHESSD
3, 4159–4187, 2015

Behavior analysis by model slope experiment of artificial rainfall

M. C. Park

Title Page
Abstract Introduction
Conclusions References
Tables Figures
◀I ▶I
◀ ▶
Back Close
Full Screen / Esc
Printer-friendly Version
Interactive Discussion

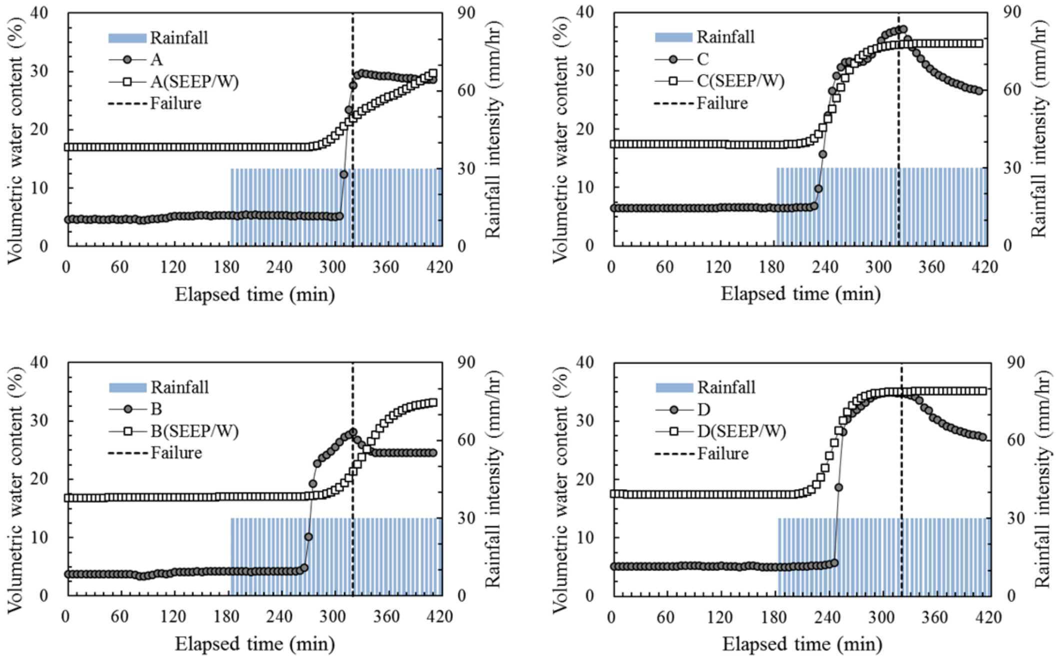

Figure 7. Comparison of experimental data and result of numerical analysis in volumetric water content.

NHESSD
3, 4159–4187, 2015

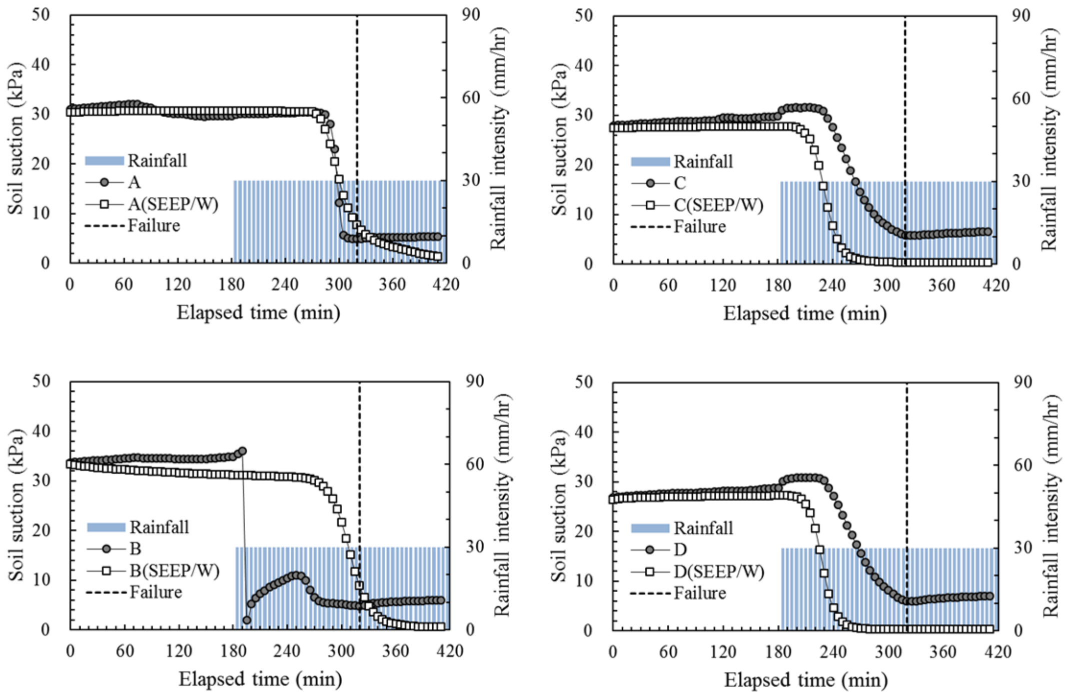

Figure 8. Comparison of experimental data and result of numerical analysis in soil suction.

NHESSD
3, 4159–4187, 2015

Title Page
Abstract
Introduction
Conclusions
References
Tables
Figures
◄
►
Back
Close
Full Screen / Esc
Printer-friendly Version
Interactive Discussion

cc BY

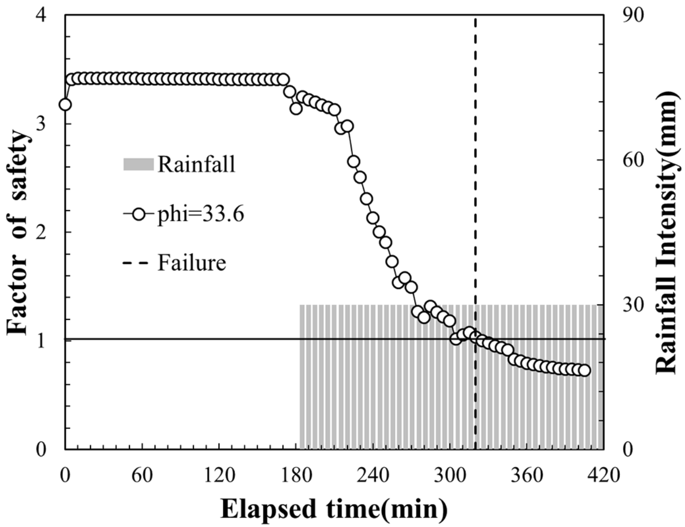

Figure 9. Factor of safety with time.

NHESSD
3, 4159–4187, 2015

CC BY

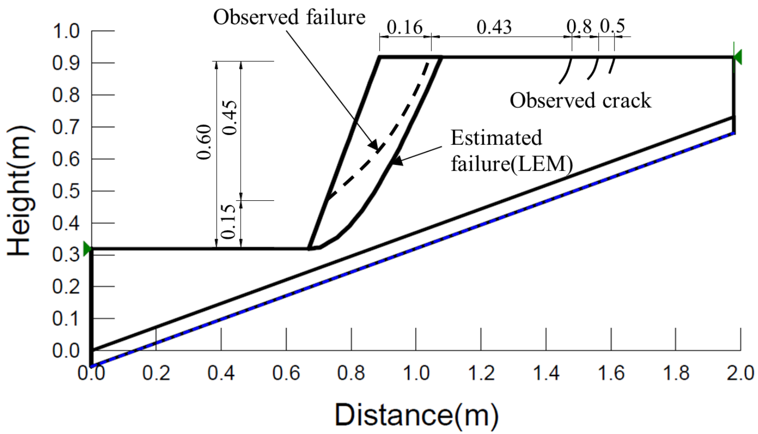

Figure 10. Comparison of failure shape.

NHESSD
3, 4159–4187, 2015

Behavior analysis by model slope experiment of artificial rainfall

M. C. Park